Structural Eng. / Earthquake Eng. Vol. 7. No. 1, 123s-131s. April 1990
Japan Society of Civil Engineers (Proc. of JSCE No. 416/I-13)

EARLY STAGE PROPAGATION BEHAVIOR OF FATIGUE CRACKS IN FILLET WELDED JOINTS

By Chitoshi MIKI, Masahiro SAKANO**, Yukihiro TOYODA*** and Tsutomu YOSHIZAWA*****

For the purpose of defining the initial crack size used in estimating the fatigue life of fillet welded joints, fatigue tests of fillet welded joints with a longitudinal attachment were carried out under constant and computer-simulated highway variable amplitude loadings, and the initiation and early-stage propagation behavior of fatigue cracks at the fillet weld toe was investigated. Facet-like fracture surfaces were observed where fatigue cracks initiated and the depth of them was independent of stress range and welding material. Fatigue life analyses applying the fracture mechanics concept were performed on the assumption that such a fracture surface is the initial crack. Good agreement was obtained between the estimated fatigue life and the experimental one.

Keywords : fatigue, fillet weld, initial crack, variable loading

1. INTRODUCTION

Fracture mechanics concept is known to be so useful in estimating fatigue life of welded joints containing discontinuities[1] that the concept of fracture mechanics has been applied to the fatigue design and fabrication of the Honshu-Shikoku bridges and other structures[2]. In fracture mechanics analyses, the initial crack size (a_i) to be assumed has a great influence on the accuracy of the estimated fatigue life. Yamada *et al.*[3,4] set the value of a_i at 0.2 mm taking account of the undercut along the weld toe, while Miki *et al.*[5~8] set at 0.02, 0.05 or 0.07 mm in consideration of correspondence between the estimated fatigue life and the experimental one of specimens. There remains ambiguity in definition of a_i at the fillet weld toe different from in the case that the obvious initial defect such as blow holes may exist. Therefore, in order to estimate fatigue life of fillet welded joints accurately, it is indispensable to define the rational value of a_i reflecting the fatigue crack initiation behavior at the weld toe.

The authors summarized fatigue cracking experiences in steel bridges and reported that fatigue crackings occured at the termination of fillet welds were the most dominant in steel bridges[9]. In this study, out-of-plane bending fatigue tests of fillet welded joints with a longitudinal attachment were carried out under constant and computer-simulated highway variable amplitude loadings, and the initiation and early-stage propagation behavior of fatigue cracks at the fillet weld toe was investigated by means of the

* Member of JSCE, Dr. Eng., Associate Professor, Department of Civil Engineering, Tokyo Institute of Technology (2-12-1, O-okayama, Meguro-ku, Tokyo 152)
** Member of JSCE, Dr. Eng., Research Associate, Department of Civil Engineering, Kansai University (3-3-35, Yamate-cho, Suita-city, Osaka 564), formerly Research Associate, Gunma University.
*** Member of JSCE, M. Eng., Research Engineer, Central Research Institute of Electric Power Industry (1646, Abiko, Abiko-city, Chiba 270-11)
**** Member of JSCE, M. Eng., Kawada Industries (Takinogawa, Kita-ku, Tokyo 114), formerly Graduate Student, Gunma University

A. C. potential drop method and the electron microfractography of fatigue failure surfaces to define the value of a_i to be used in fatigue life analyses. Fatigue specimens were welded using six kinds of electrodes since welding materials were expected to have some influence on small crack initiation and propagation behavior in the vicinity of the weld toe. The validity of the defined value of a_i was verified by comparing the estimated fatigue life with the experimental one.

2. FATIGUE TEST PROCEDURE

(1) Specimen

Configurations and dimensions of the fillet welded specimen with a longitudinal attachment are shown in Fig. 1. Specimens were made of JIS SM 50 YA, whose mechanical properties and chemical composition are given in Table 1. Six kinds of welding electrodes used for fabricating specimens are the following : A 1, A 2, A 3 (low-hydrogen type electrode ; JIS D 5016), B (low-hydrogen type electrode for fillet welding ; JIS D 5026), C (solid wire for CO_2 arc welding ; JIS YCW 1), and D (flux-cored wire for CO_2 arc welding ; JIS YFW 24). These symbols of welding electrodes also represent the kinds of specimens. Vickers hardness (5 kg-weight) is, independent of welding materials, 260-320 in weld metal, 320-380 in heat-affected zone, and 190-220 in base metal.

(2) Fatigue test method

Fatigue tests were performed under constant and variable amplitude four-points out-of-plane bending as shown in Fig. 1 by an electro-hydraulic fatigue testing machine. Fatigue behavior of this type of joint under out-of-plane bending has scarcely investigated in the past. The rate of stress repetition was 10-30 Hz. The maximum value of nominal bending stress at the weld toe was set at 250 MPa (about 65 % of the yield strength of the SM 50 steel) for all of the specimens, considering the hypothesis[10] that the maximum value

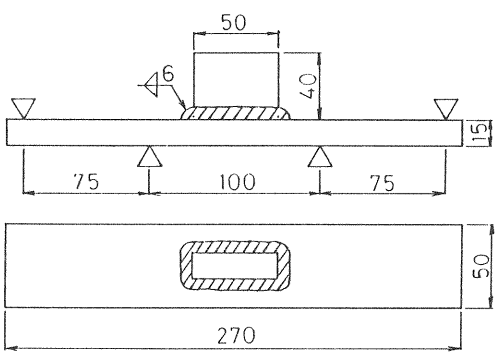

Fig. 1 Four-point Bending Specimen (Dimensions are in mm).

Table 1 Mechanical Properties and Chemical Composition of SM 50 Steel.

Mechanical Properties			Chemical Composition (%)					
Y.P. (MPa)	T.S. (MPa)	EL. (%)	C x100	Si	Mn	P x1000	S	Cu
390	560	25	17	45	147	21	7	10

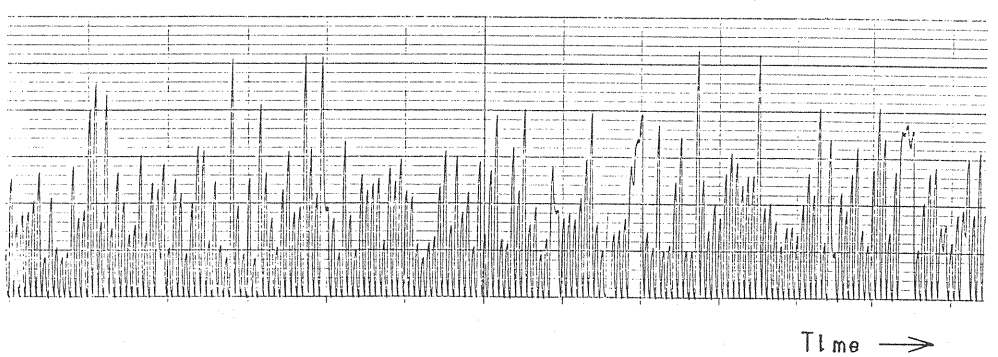

Fig. 2 Example of Variable Amplitude Loading Waveform.

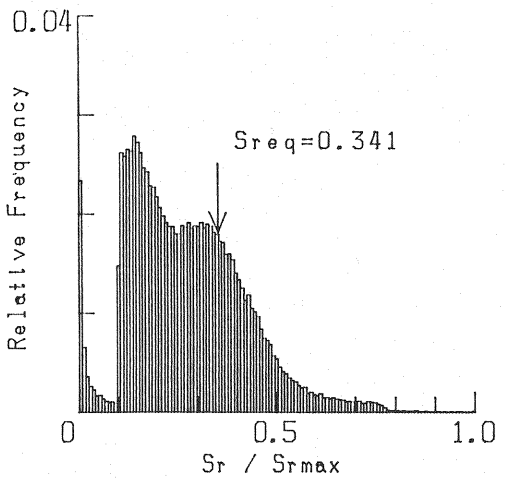

Fig. 3 Variable Amplitude Stress Range Histogram.

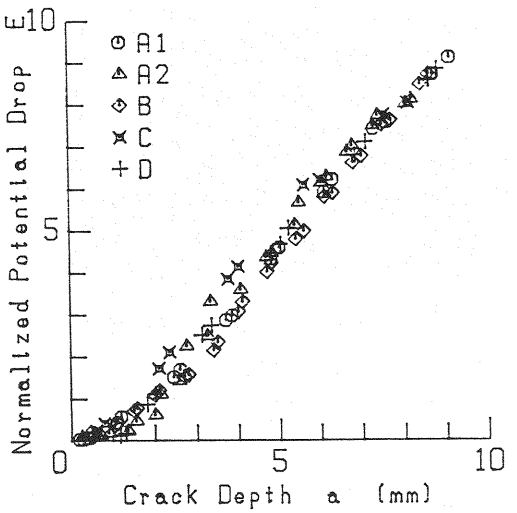

Fig. 4 Relationship between Crack Depth and Normalized Potential Drop.

of stress fluctuation might be raised to the yield strength of the material by tensile residual stresses in full-sized welded joints.

In variable amplitude loading tests, the computer-simulated highway bridge stresses[11] were used as the stress waveform. Fig. 2 shows some parts of the stress waveform, and Fig. 3 shows the normalized stress range histogram counted by the rainflow method. The ratio of the equivalent stress range (S_{req}) obtained as the root-mean-cube value of all stress ranges to the maximum stress range (S_{rmax}) is 0.341. In the previous study[8], stress fluctuations below the 40 % of S_{rmax} were deleted for the purpose of saving time required for fatigue tests. In this study, the deleting revel of lower stresses is set to be 10 % in order to investigate the effect of lower stress fluctuations. Variable amplitude loading tests were performed using only B-type specimens.

(3) Detection of fatigue cracks

The alternating current potential drop method was applied to detecting fatigue cracks. Fig. 4 shows the relationship between crack depth and normalized potential drop obtained through beach mark tests for each type of specimens. Although some scatter is observed, fatigue cracks of 0.3-0.5 mm depth could be detected by use of this method. In this study, fatigue crack initiation life (N_c) is defined to be the number of stress cycles when a crack of 1 mm depth is detected, because of the reliance of crack size measuring.

3. FATIGUE TEST RESULTS

Fatigue cracks initiated from the fillet weld toe at the longitudinal attachment end and propagated into the base plate as the semi-elliptical shaped crack as shown in Fig. 5. Fig. 6 shows fatigue test results under constant and variable amplitude loadings. Constant amplitude fatigue test results are plotted with fatigue crack initiation life (N_c) and fatigue failure life (N_f) as abscissa against nominal bending stress range (S_r) as ordinates, and variable amplitude fatigue test results are plotted with N_c and N_f as abscissa against equivalent stress range (S_{req}) as ordinates. S_{req} is obtained as the root-mean-cube value of all S_r in variable amplitude stresses.

Under constant amplitude loading, S_r vs. N_c and S_r vs. N_f relationships of the failed specimens are roughly represented by a straight line respectively regardless of welding materials, though N_c is rather widely scattered than N_f owing to the aberration of the potential drop method. The solid line shown in Fig. 6 is a regression line of S_r vs. N_f relationship of the failed specimens expressed by Eq. (1), and the broken line is a regression line of S_r vs. N_c relationship expressed by Eq. (2).

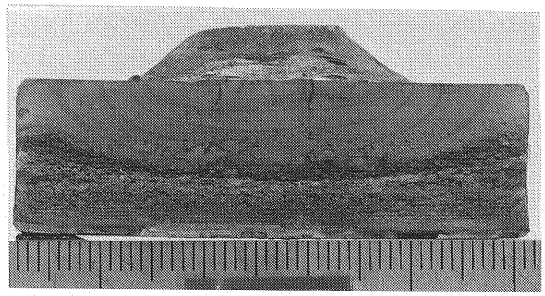

Fig. 5 Fracture Surface (D-type, S_r=225 MPa).

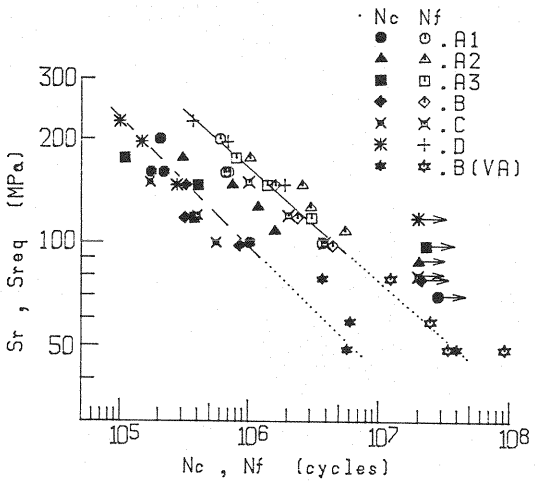

Fig. 6 Fatigue Test Results under Constant and Variable Amplitude Loading.

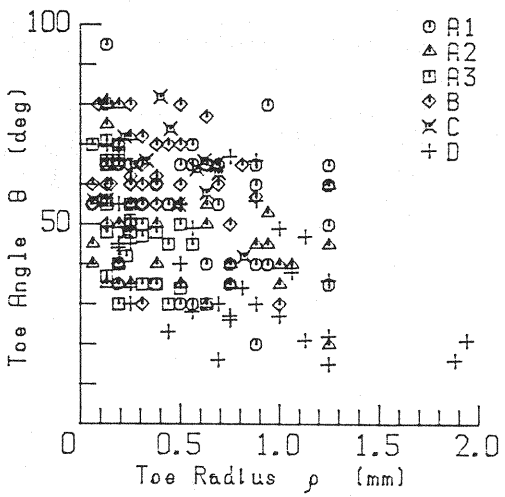

Specimen Type	ρ mean (mm)	θ mean (deg)
A1	0.62	54
A2	0.51	52
A3	0.26	50
B	0.38	61
C	0.43	62
D	0.93	37

Fig. 7 Distribution of Toe Angle and Toe Redius.

$$S_r^{2.98} \cdot N_f = 4.21 \times 10^{12} \quad (1)$$

$$S_r^{2.58} \cdot N_c = 1.25 \times 10^{11} \quad (2)$$

The mark with an arrow in Fig. 6 indicates the specimen in which no fatigue cracks were detected by the a. c. potential drop method after stress repetitions of more than 2×10^7 cycles. Fatigue limit of each type of specimen exists between such a non-cracking stress range and the lowest cracking stress range. On comparing these stress ranges, it is obvious that fatigue limit of D-type specimen is higher than that of the other types of specimens. The fatigue strength of B-type specimens for which so-called improved electrode is applied is same as others. Fig. 7 shows the distribution of the toe angle and the toe radius measured near the crack initiation point and the average values of them for each specimen. As shown in Fig. 7, toe angle is smaller and toe radius is larger in the D-type specimen than those in the other specimens. Fig. 8 illustrates fillet weld toe macrosections of typical specimens. The local configuration of weld toe of D-type specimen is gentler than that of the other specimens. As mentioned above, the local configuration of weld toe where fatigue cracks initiate have some influence on the long life fatigue strength of fillet welded joints.

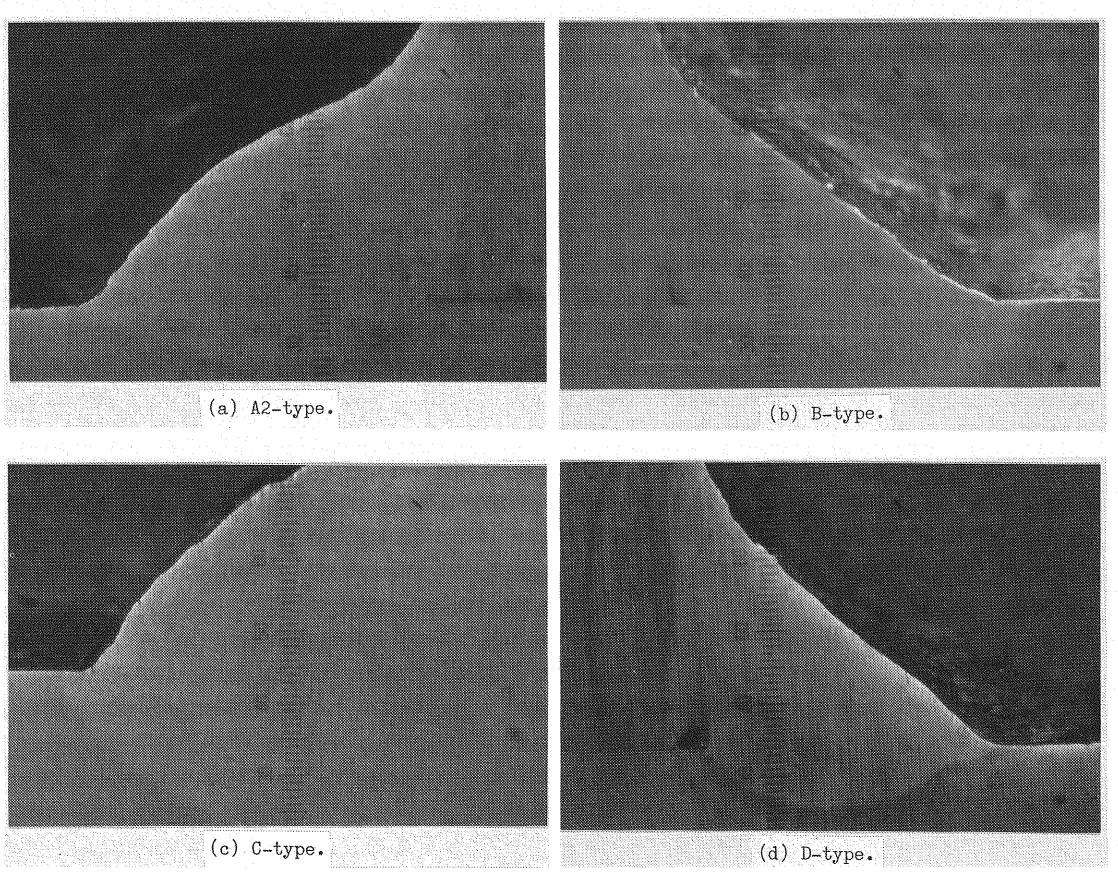

Fig. 8 Macrosection of Fillet Weld Toe.

Variable amplitude fatigue test results of S_{req} larger than 60 MPa are plotted approximately on extensions of constant amplitude S_r-N_c and S_r-N_f lines (dotted lines shown in Fig. 6) similarly to the case of the cruciform welded joint reported by the authors[8], whereas some results of S_{req} smaller than 50 MPa are located on the longer life side of extensions of those regression lines. Hence, fatigue life estimation applying the modified Miner's rule is too conservative under variable loadings including numerous lower stress cycles. These low-stress and long-life fatigue test data could not obtained in the previous study[8], which are of great use for evaluating fatigue life under actual variable stresses.

Fig. 9 shows S_r vs. N_c/N_f relationship and S_{req} vs. N_c/N_f relationship. It requires 10-40 % of N_f for fatigue cracks of 1 mm depth to develop independent of S_r or S_{req} under both of constant and variable amplitude loadings.

4. DISCUSSION ON INITIAL CRACK SIZE

(1) Fractographic analysis

Fig. 10 shows scanning electron micrographs of fatigue fractured surfaces near the crack initiating point. Facet-like portions in contact with the surface as shown in the figures were observed where fatigue cracks started to propagate in all specimens failed under constant or variable amplitude loading. Kobayashi *et al.*[12] observed similar facet-like fracture surfaces in low-carbon steel unnotched specimens subjected to stress repetitions near the fatigue limit whether failed or unfailed, and considered such a fracture surface to be a stage I crack surface. Tanaka and Akiniwa[13] reported that the depth of such a shear mode fracture surface observed in SM 41 notched specimens was independent of notch geometry and stress amplitude, and that the average size of them was about 0.06 mm.

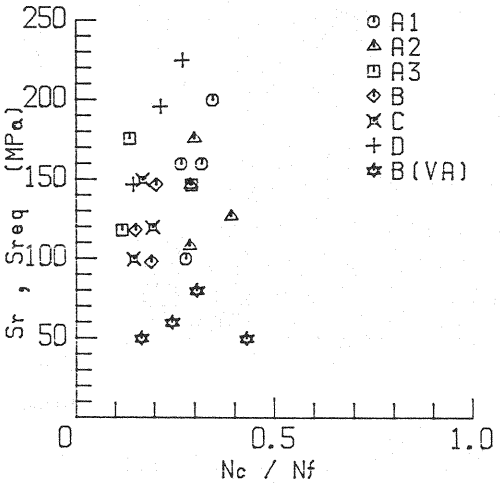

Fig. 9 Ratio of N_c to N_f.

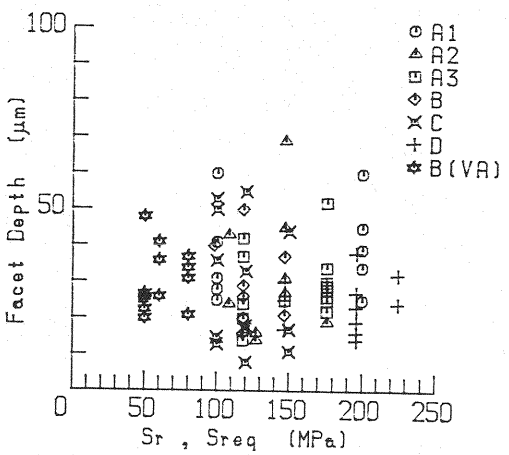

Fig. 11 Depth of Facet-like Fracture Surfaces.

Fig. 11 shows the relationship between the depth of facet-like fracture surface and the stress range. The depth of facet-like fracture surfaces varies within the range of 0.01-0.07 mm roughly independent of stress range, welding material, and stress history. The mean value of them is 0.03 mm. In this study, we assumes the initial crack depth to be 0.03 mm, because these facet-like fracture surface are considered to develop at an extremely early stage of fatigue life (less than 10 % of N_f), and because the depth of them can be regarded as a characteristic value of the 490 MPa-class weldment.

(2) Fatigue crack propagation life analysis

In order to verify the validity of the assumption on the initial crack size mentioned in the section 4. (1),

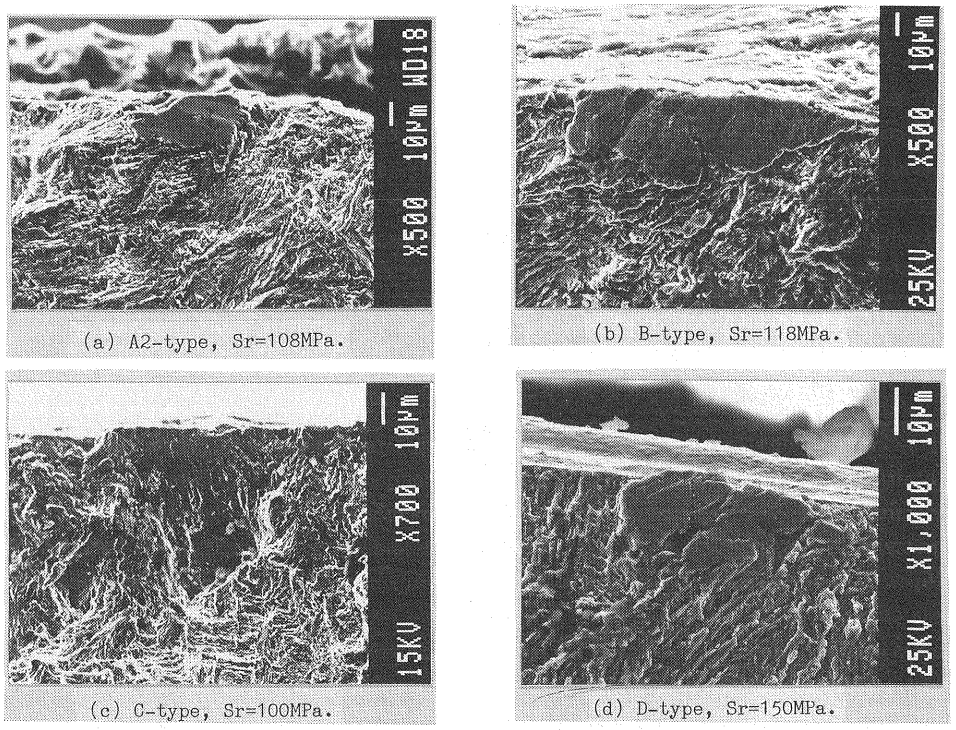

Fig. 10 Scanning Electron Micrograph of Fatigue Fracture Surface.

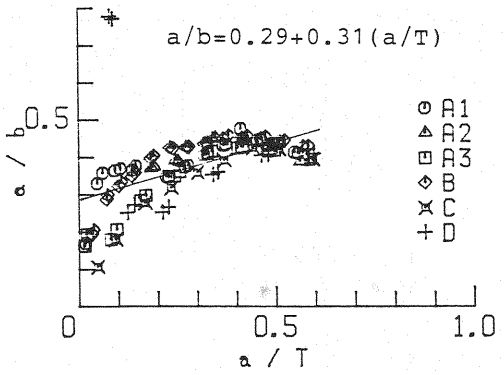

Fig. 12 Change of Crack Aspect Ratio with Crack Depth.

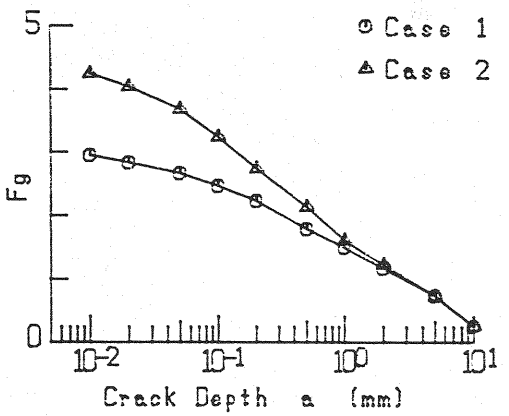

Fig. 13 Change of Correction Factor F_g with Crack Depth.

fatigue crack propagation analysis applying the fracture mechanics concept was performed and the estimated fatigue life was compared with the experimental value. The final crack depth was assumed to be 1 mm for N_c and 60 % of the plate thickness for N_f on basis of the observation of failed cross sections.

The stress intensity factor range (ΔK) for a semi-elliptical surface crack initiated at the weld toe is expressed by Eq. (3)

$$\Delta K = S_r\sqrt{\pi a}\cdot F_s\cdot F_g \quad \cdots\cdots (3)$$

where a is crack depth, F_s is a correction factor for effects of the crack shape and dimensions of the cross section, and F_g is one for effects of the geometrical stress concentration. F_s is calculated by Eq. (4)[14]

$$F_s = 1/E(k)\cdot\{M_1+M_2(a/T)^2+M_3(a/T)^4\}\sqrt{\sec(\pi b/W\sqrt{a/T})} \quad \cdots\cdots (4)$$

$$E(k)=\sqrt{1+1.464(a/b)^{1.65}}$$

$$M_1=1.13-0.09(a/b)$$

$$M_2=-0.54+0.89/(0.2+a/b)$$

$$M_3=0.5-1/(0.65+a/b)+14(1-a/b)^{24}$$

where b is half of the crack surface length, W is the plate width, and T is the plate thickness. The aspect ratio of crack (a/b) is assumed to vary with the normalized crack depth (a/T). Fig. 12 shows the relationship between a/b and a/T obtained by beach mark tests.

The value of F_g can be obtained from the stress intensity factor for a crack subjected to the stress distribution occurred when no cracks exist[15]. The stress distribution without cracks was computed by the 3-dimensional FEM[16]. In the FEM analysis, the toe radius and the toe angle were assumed to be following two cases : case 1 ; 1.0 mm and 35 deg., case 2 ; 0.5 mm and 55 deg.. Case 1 corresponds to D-type specimen, and case 2 corresponds to the other 5 types of specimens in average. Fig. 13 shows the change of F_g with the crack depth. Since there is little difference between case 1 and case 2 for the crack depth more than 1 mm, the extent under the influence of the local configuration of weld toes from the surface is 1 mm at most.

Fatigue crack growth rate (da/dN) vs. ΔK relationship expressed by Eq. (5)

$$da/dN = 5.0\times10^{-12}\cdot\Delta K^3 \quad (\Delta K > \Delta K_{th}) \quad \cdots\cdots (5)$$

which was obtained by Okumura *et al.*[17] as an average value for structural steels was used. The threshold value (ΔK_{th}) was assumed to be 2.5 MPa$\sqrt{m}$ obtaind by NRIM[18] for welded joints. In estimating fatigue life under variable amplitude loading, the hypothesis[19] that fatigue cracks could be propagated only by ΔK exceeding ΔK_{th} was applied.

Fig. 14 shows estimated lines and experimental values of N_c and N_f under constant and variable amplitude loadings. Since estimated lines correspond to experimental values, the assumption of the initial crack size has been confirmed to be appropriate.

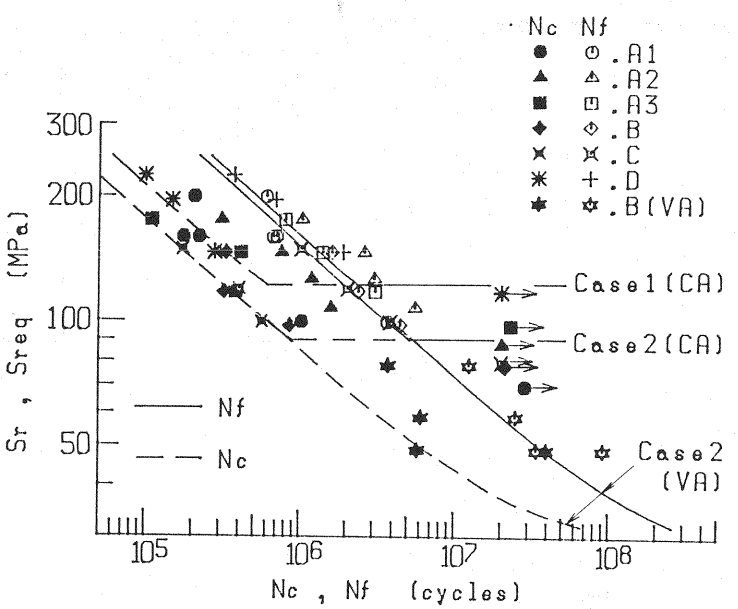

Fig. 14 Comparison of Estimated Fatigue Life Curves with Experimental Results.

5. CONCLUDING REMARKS

The initiation and early stage propagation behavior of fatigue cracks at the fillet weld toe was observed and the initial crack size used in fracture mechanics fatigue life analyses were examined. The following is the principal results obtained from this study :

(1) Fatigue cracks initiated from the weld toe at the longitudinal attachment end and propagated in semi-elliptical shapes. The fatigue limit of the specimen welded by a flux-cored wire for CO_2 arc welding was higher than that of the other types of specimens, because the local configuration of the weld toe of that type of specimen was gentler than that of the others.

(2) Some of variable amplitude fatigue test results in the low stress region were located on the longer life side of the extension of constant amplitude regression lines in the S-N diagram.

(3) Facet-like fracture surfaces in contact with the surface were observed where fatigue cracks initiated in all specimens failed under constant and variable amplitude loadings. The depth of such a fracture surface varied within the range of 0. 01-0. 07 mm roughly independent of stress range, welding material, and stress history.

(4) The assumption that a facet-like fracture surface is the initial crack has been confirmed to be appropriate on comparing the estimated fatigue life with the experimental one under constant and variable amplitude loadings.

ACKNOWLEDGMENT

The authors would like to thank Dr. Takeshi Mori and Mr. Miyabu Kouno fo Tokyo Institute of Technology and Mr. Masashi Ikeda of Gunma University for their invaluable advice and assistance. Stress analysis was performed using the Computer Center of Gunma University. This study was supported in part by the Grant-in-Aid for General Scientific Research from the Japanese Ministry of Education, Science and Culture (No. 01550362).

REFERENCES

1) Committee on Structural Engineering, Structural Mechanics, Fracture Mechanics : Application of Fracture Mechanics to Civil

Engineering Problems, Proc. of JSCE, No. 380/I-7, pp. 13~26, 1987 (in Japanese).
2) Kubomura, K., Shimokawa, H. and Takena, K. : Development of Technology to Construct Long Span Bridges for Combined Use of Highway and Railway, Journal of JSCE, Vol. 68-7, pp. 18~27, 1983 (in Japanese).
3) Yamada, K. and Hirt, M. A. : Parametric Fatigue Analysis of Weldments using Fracture Mechanics, Proc. of JSCE, No. 319, pp. 56-64, 1982 (in Japanese).
4) Tagaki, N., Kondo, A., Yamada, K. and Kikuchi, Y. : Effect of Weld Toe Profiles on Fatigue Strength of Fillet Welded Specimens, Proc. of JSCE, No. 324, pp. 151-159, 1982 (in Japanese).
5) Miki, C., Mori, T., Sakamoto, K. and Kashiwagi, H. : Size Effect on the Fatigue Strength of Transverse Fillet Welded Joints, Journal of Structural Engineering, Vol. 33 A, pp. 393-402, 1987 (in Japanese).
6) Miki, C., Mori, T., Tuda, S. and Sakamoto, K. : Retrofitting Fatigue-cracked Joints by TIG Arc Remelting, Structural Eng./Earthquake Eng., Vol. 4, No. 1, pp. 85 s-93 s, 1987.
7) Takena, K., Kawakami, H., Itoh, F. and Miki, C. : Stress Analysis and Calculation of Fatigue Lives about Web-gusset Welded Joints, Proc. of JSCE, No. 392/I-9, pp. 345-350, 1988 (in Japanese).
8) Miki, C., Murakoshi, J., Toyoda, Y. and Sakano, M. : Long Life Fatigue Behavior of Fillet Welded Joints under Computer Simulated Highway and Railroad Loading, Structural Eng./Earthquake Eng., Vol. 6, No. 1, pp. 41 s-48 s, 1989.
9) Miki, C., Sakano, M., Tateishi, K. and Fukuoka, Y. : Data Base for Fatigue Crackings in Steel Bridges, Proc. of JSCE, No. 392/I-9, pp. 403-410, 1988 (in Japanese).
10) Nakamura, H. *et al.* : A Method for Obtaining Conservative *S-N* Data for Welded Structures, J. Testing and Evaluation, Vol. 16, No. 3, pp. 280-285, 1988 (in Japanese).
11) Miki, C., Goto, Y., Yoshida, H. and Mori, T. : Computer Simulation Studies on the Fatigue Load and Fatigue Design of Highway Bridges, Structural Eng./Earthquake Eng., Vol. 2, No. 1, pp. 13 s-22 s, 1985.
12) Kobayashi, H., Kawada, Y. and Nakazawa, H. : A Fractographic Study of Stage I Cracking with Particular Reference to Endurance Limit, J. JSMS, Vol. 25, No. 276, pp. 881-887, 1976 (in Japanese).
13) Tanaka, K. and Akiniwa, Y. : Resistance-curve Method for Predicting Propagation Threshold of Short Fatigue Cracks at Notches, Engineering Fracture Mechanics, Vol. 30, No. 6, pp. 863-876, 1988.
14) The Society of Materials Science, Japan : Stress Intensity Factors Handbook, Vol. 2, pp. 712-722, Pergamon Press, 1987.
15) Okamura, H. : Introduction to Linear Fracture Mechanics, Baifukan, 1976 (in Japanese).
16) Wilson, E. L. : A Static Analysis Program for Three Dimensional Solid Structures, Denver Mining Research Center Report, U. S. Department of the Interior Bureau of Mines, 1971.
17) Okumura, T., Nishimura, T., Miki, C. and Hasegawa, K. : Fatigue Crack Growth Rates in Structural Steels, Proc. of JSCE, No. 322, pp. 175-178, 1981.
18) National Research Institute for Metals (Japan) : Fatigue Data Sheets, No. 21, 1980 and No. 31, 1982 (in Japanese).
19) Miki, C., Murakoshi, J. and Sakano, M. : Fatigue Crack Growth in Highway Bridges, Structural Eng./Earthquake Eng., Vol. 4, No. 2, pp. 371 s-380 s, 1987.

(Received October 23 1989)